WARSAW UNIVERSITY OF TECHNOLOGY
FACULTY OF ELECTRONICS
AND INFORMATION TECHNOLOGY
INSTITUTE OF RADIOELECTRONICS

Report No. 2, 2014

Quaternion polar representation in analysis of brightness of color images

by

Kajetana M. Snopek, Natalia M. Zienkowicz

Warsaw, July 2014

QUATERNION POLAR REPRESENTATION IN ANALYSIS OF BRIGHTNESS OF COLOUR IMAGES

Kajetana M. Snopek, Natalia M. Zienkowicz

Warsaw University of Technology, Poland

ABSTRACT

The paper presents basic results of the preliminary research concerning application of quaternion polar representation in analysis of colour images. Three test images (RGB) of diverse complexity have been examined. In the hypercomplex domain they are represented by a normalized reduced quaternion. Its polar form is given by Euler's angles defined according to the XZY–convention. The quaternion polar form has been used to observe the effects of changes in brightness of test images. The measure of this deformation is the difference between Euler's angles of distorted and original images. The paper is illustrated with numerous figures.

Index Terms— quaternion polar representation, Euler's angles, RGB images, brightness

1. INTRODUCTION

Quaternions form the algebra of order 4 over the real numbers field $\mathbb{R}$. Sangwine was the first to interpret the vector part of a quaternion in terms of three components: R (red), G (green) and B (blue) of a colour image [1]. This let to develop some advanced methods of decomposition and compression, pattern recognition, edge detection [2–7], as well as to elaborate novel hypercomplex filtering and watermarking methods [8–11]. In the last few years quaternions have also proliferated into domain of the wavelet transformation [12–13]. They provide a convenient notation for representing movement of a rigid body in 3-D space. In consequence, they are effectively applied in computer graphics, computer vision and robotics, astrophysics and in theoretical physics [14–18].

Having in mind the expected future applications of quaternions in correction of colour images, this paper is devoted to analysis of the influence of brightness changes on quaternion polar form of colour images. The next section presents the theoretical basis of the research.

2. THEORETICAL BACKGROUND

Consider a colour (RGB) image written as a *reduced quaternion*

$$q = Ri + Gj + Bk \tag{1}$$

where R represents a red component, G – a green one and B – a blue one. The imaginary units i, j, k satisfy Hamiltonian multiplication rules [19]. The norm of (1) is given by

$$|q| = \sqrt{R^2 + G^2 + B^2}. \tag{2}$$

In colour image analysis, we apply *reduced normalized* quaternions of norm equal 1, i.e.,

$$q_{norm} = \frac{q}{|q|} = \frac{Ri+Gj+Bk}{\sqrt{R^2+G^2+B^2}} \Rightarrow |q_{norm}| = 1. \tag{3}$$

According to the XZY-convention, the normalized quaternion q_{norm} (of norm =1) can be represented in an equivalent polar form [20] as follows

$$q_{norm} = e^{i\phi} e^{k\psi} e^{j\theta} \tag{4}$$

where $\phi, \theta, \psi \in [-\pi, \pi[\times [-\pi/2, \pi/2[\times [-\pi/4, \pi/4]$ are Euler's angles. This convention describes rotation of the 3–D Cartesian coordinate system (x, y, z) by angles ϕ, ψ, θ around axes Ox, Oz, Oy respectively. The matrix $M_{3\times3}$ of this rotation is

$$M = \begin{bmatrix} \cos\theta\cos\psi & -\sin\theta & \cos\theta\sin\psi \\ \sin\varphi\sin\psi + \cos\varphi\sin\theta\cos\psi & \cos\varphi\cos\theta & -\sin\varphi\cos\psi + \cos\varphi\sin\theta\sin\psi \\ \cos\varphi\sin\psi - \sin\varphi\sin\theta\cos\psi & \sin\varphi\cos\theta & \cos\varphi\cos\psi + \sin\varphi\sin\theta\sin\psi \end{bmatrix} \tag{5}$$

Its equivalent form expressed in terms of imaginary components of (1) is

$$M = \begin{bmatrix} R^2 - G^2 - B^2 & 2RG & 2RB \\ 2RG & -R^2 + G^2 - B^2 & 2GB \\ 2RB & 2GB & -R^2 - G^2 + B^2 \end{bmatrix} \tag{6}$$

Comparing (5) and (6), the relations are following:

$$\cos\theta\cos\psi = R^2 - G^2 - B^2, \tag{7}$$

$$-\sin\theta = 2RG, \tag{8}$$

$$\cos\theta\sin\psi = 2RB, \tag{9}$$

$$\sin\varphi\sin\psi + \cos\varphi\sin\theta\cos\psi = 2RG, \tag{10}$$

$$\cos\varphi\cos\theta = -R^2 + G^2 - B^2, \tag{11}$$

$$-\sin\varphi\cos\psi + \cos\varphi\sin\theta\sin\psi = 2GB, \tag{12}$$

$$\cos\varphi\sin\psi - \sin\varphi\sin\theta\cos\psi = 2RB, \tag{13}$$

$$\sin\varphi\cos\theta = 2GB, \tag{14}$$

$$\cos\varphi\cos\psi + \sin\varphi\sin\theta\sin\psi = -R^2 - G^2 + B^2. \tag{15}$$

The above Eqs. (7)–(15) serve to develop three Euler's angles in terms of RGB–components as follows

$$\varphi = \tan^{-1}\frac{2GB}{-R^2+G^2-B^2}, \tag{16}$$

$$\theta = \tan^{-1}\frac{-2RG}{\sqrt{1-2R^2G^2}}, \tag{17}$$

$$\psi = \tan^{-1}\frac{2RB}{R^2-G^2-B^2}. \tag{18}$$

Reciprocally, from (7)–(15) we can derive *reconstruction formulas* for components R, G, B of colour images, as follows

$$R = \sin\frac{\varphi}{2}\cos\frac{\theta}{2}\cos\frac{\psi}{2} - \sin\frac{\theta}{2}\sin\frac{\psi}{2}\cos\frac{\varphi}{2}, \tag{16}$$

$$G = -\sin\frac{\varphi}{2}\cos\frac{\psi}{2}\sin\frac{\theta}{2} + \cos\frac{\theta}{2}\cos\frac{\varphi}{2}\sin\frac{\psi}{2}, \tag{17}$$

$$B = \sin\frac{\varphi}{2}\cos\frac{\theta}{2}\sin\frac{\psi}{2} + \cos\frac{\psi}{2}\cos\frac{\varphi}{2}\sin\frac{\theta}{2}. \tag{18}$$

3. DESCRIPTION OF THE EXPERIMENT

A test RGB image (original) has been lightened or darkened to get a "distorted" image (R'G'B') as shown in Fig. 1. Both images are respectively represented by quaternions q and q' of the form (1). Then, using (16)–(18), the difference between Euler's angles φ, θ, ψ of both images is calculated and visualized in the form of images.

4. TEST IMAGES

Having in mind their diverse complexity, three test images have been chosen. The first one "simple.bmp" (I) (Fig. 2a) represents a palette of 27 colours with RGB-values from a set {0, 128, 255}. For convenience, all colours have been enumerated with successive numbers from 1 to 27. We see that for $R = G = B = 0$, we have a black colour (No. 1), while $R = G = B = 255$ represent a white one (No. 27). The same colours appear in the test image II "rainbow.bmp" (Fig. 3a) showing a series of ribbons with well visible edges and shadows. The last test image III "swan.bmp" (Fig. 4a) is a real colour picture representing a swan's head. All images have been lightened (Figs 2b, 3b, 4b) and darkened (Figs 2c, 3c, 4c) by subtracting or adding 60 to RGB-values of each pixel. Then, the influence of these changes on phase angles ϕ, θ, ψ of a given image has been studied. In the next Section, let us present the results of this experiment.

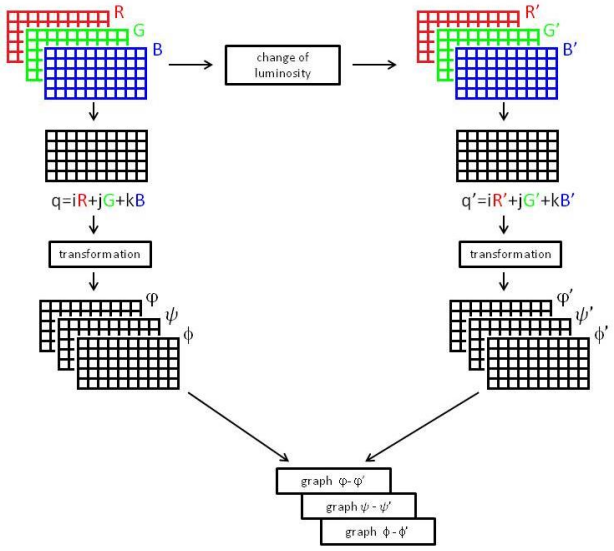

Fig. 1. Scheme representing the experiment.

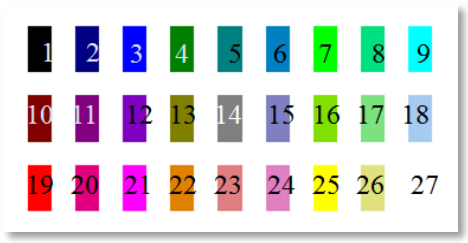

(a) The original image

(b) The lightened image

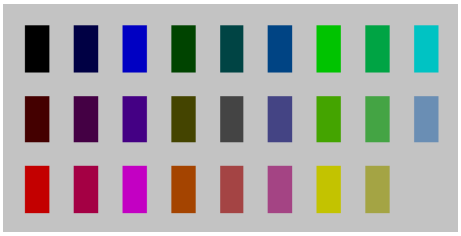

(c) The darkened image

Fig. 2. Test image I "simple.bmp".

(a) The original image

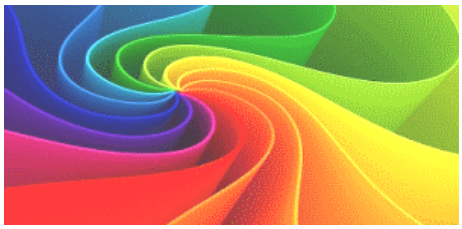

(b) The lightened image

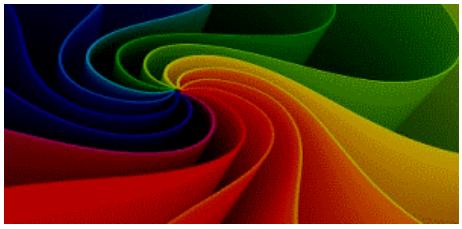

(c) The darkened image

Fig. 3. Test image II"rainbow.bmp".

(a) The original image

(b) The lightened image

(c) The darkened image

Fig. 4. Test image III "swan.bmp".

5. EXPERIMENTAL RESULTS

Using the computer program elaborated in Matlab and the theoretical formulas (16)–(18), the values of Euler's angles ϕ, θ, ψ representing three phases of a colour image have been calculated.

5.1. Influence of changes in brightness on the angle ϕ

Studying the influence of lightening of the test image I (Fig. 2a) on the angle ϕ, the biggest difference has been noticed for colours No. 1, 13 and 25. While the image was darkened, the changes appeared visibly for colours No. 6, 8, 17, 23, 24. The same property has been observed for more complicated images (II, III). Next Figs 5 and 6 show the influence of the brightness changes on the angle ϕ. For the lightened image, the values of the phase ϕ oscillated between –0,55 and 0,65 [rad]. The change of brightness affects most the angle ϕ for green and yellow colours (Fig. 5). For the darkened image, the biggest difference between phases (equal –1,5 rad) has been noted for the shadow part between rose and violet ribbons. Similarly, the value of ϕ decreases by 0,5[rad] for the shadow part between light blue and green ribbons of the original image.

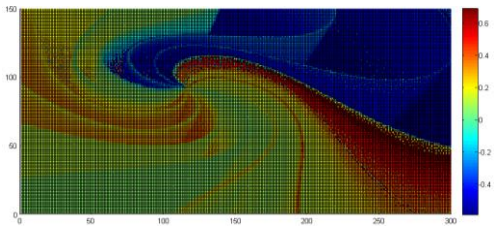

Fig. 5 The influence of lightening on the angle ϕ of the test image II

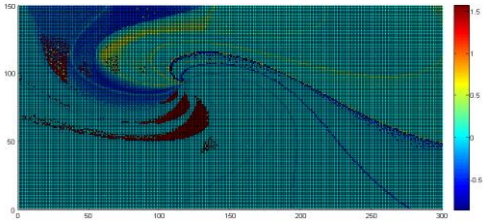

Fig. 6 The influence of darkening on the angle ϕ of the test image II

Next Fig. 7 shows the influence of the lightening on the phase angle ϕ of the test image "swan.bmp". The difference is especially noticeable for red colours of the original image. The darkening of the image (Fig. 8) influences considerably the background part of the original image. We also observed the slight shadows, not visible in the original black background (Fig. 4a).

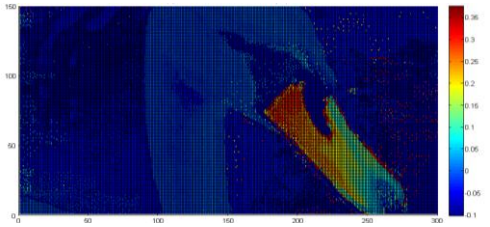

Fig. 7 The influence of lightening on the angle ϕ of the test image III

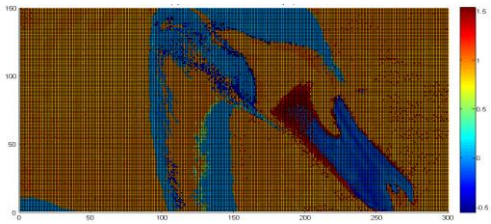

Fig. 8 The influence of darkening on the angle ϕ of the test image III

5.2. Influence of changes in brightness on the angle θ

The lightening of the test image "simple.bmp" influences most the angle θ for colours No. 1, 4, 10. In the darkened image, the biggest difference has been observed for colours No. 16, 22 i 26. Observing the influence of the lightening of the test image II on θ, we see that it affected all colours, especially in the shadow regions of the original image. Let us suppose that this property could serve to eliminate redundant shadows in the original image. Differently, the darkening of the test image II affected most the green colours (see the top right part of Fig. 3a), as shown in Fig. 9. For other colours, the differences between phase angles θ were approximately zero. Let us also notice that, contrary to Fig. 6, the edges representing transitions between successive rainbow colours are well visible in both cases. The lightening of the test image III affected the whole image, as it is seen in Fig. 11. However, the most dynamic change is observed for the black background of the original. It is not observed in the case of darkening (Fig. 12).

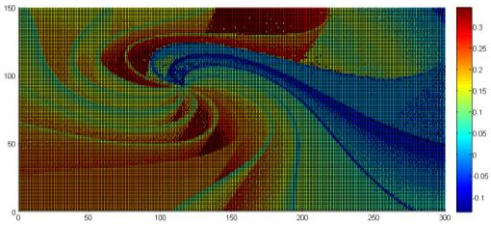

Fig. 9 The influence of lightening on the angle θ of the test image II

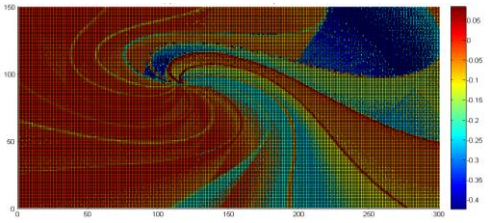

Fig. 10 The influence of darkening on the angle θ of the test image II

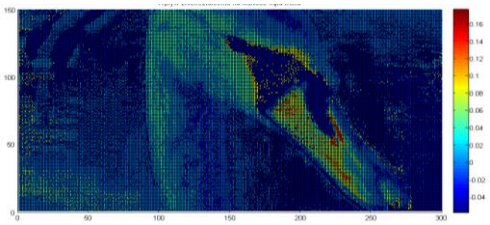

Fig. 11 The influence of lightening on the angle θ of the test image III

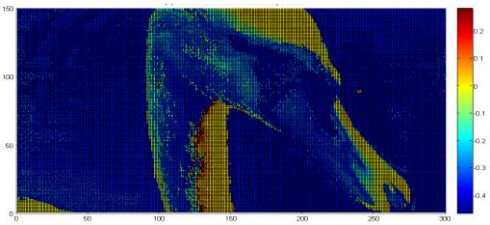

Fig. 12 The influence of darkening on the angle θ of the test image III

5.3. Influence of changes in brightness on the angle ψ

Testing the changes in ψ for "simple.bmp", it has been noted that colours No. 1, 13 and 25 are the most sensitive on lightening, similarly as it was described in Section 5.1. For the darkened image, the biggest differences between phases was observed for colours No. 17, 20 and 23. The Fig. 13 shows the difference between phase angles ψ of the original and lightened image "rainbow.bmp". The curve separating "warm" and "cold" colours has appeared. Differently, in Fig. 14 we notice the slight influence of the darkening on the violet colour. Comparing the effects of lightening (Fig. 15) and darkening (Fig. 16) of the test image "swan.bmp", the well visible contour of the swan's neck in the last case is noticed. Differently, on Fig. 15 the neck is completely fused with the background.

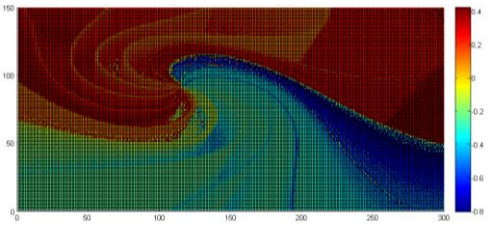

Fig. 13 The influence of lightening on the angle ψ of the test image II

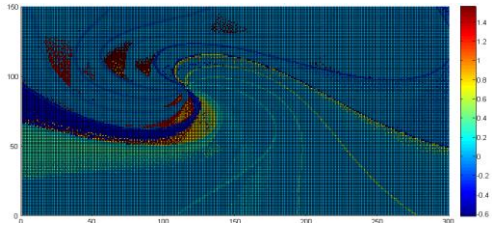

Fig. 14 The influence of darkening on the angle ψ of the test image II

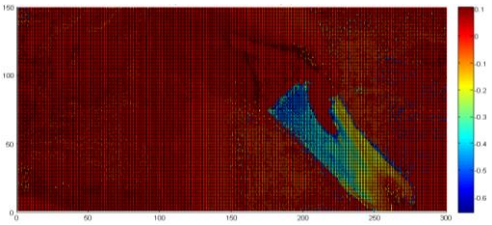

Fig. 15 The influence of lightening on the angle ψ of the test image III

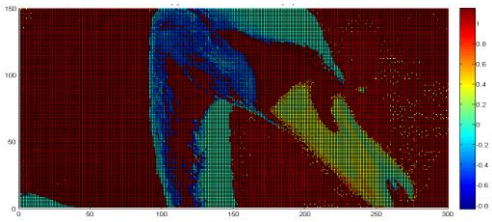

Fig. 16 The influence of darkening on the angle ψ of the test image III

5. SUMMARY

The results of the preliminary research concerning the influence of different changes in colour images on its phase angles have been presented. It has been observed how the phases of a colour image represented as Euler's angles react on brightness changes. Some interesting observations have been made that can be useful in colour image correction or in spectrometry.

10. REFERENCES

[1] S.J. Sangwine, "Fourier transforms of colour images using quaternion or hypercomplex numbers," *Electron. Lett.*, vol. 32, no. 21, pp. 1979-1980, Oct. 1996.

[2] N. Le Bihan, S.J. Sangwine, "Color Image Decomposition Using Quaternion Singular Value Decomposition," Intern. Conf. on Visual Information Engineering, July 7-9, 2003, pp. 113-116.

[3] D.S. Alexiadis, G.D., "Estimation of Motions in Color Image Sequences Using Hypercomplex Fourier Transforms," *IEEE Trans. Image Processing*, vol. 18, no. 1, pp. 168-187, January 2009.

[4] S.-C. Pei, J.-J. Ding, J.Chang, "Color pattern recognition by quaternion correlation," IEEE Int. Conf. Image Process., Thessaloniki, Greece, October 7-10, 2010, pp. 894-897

[5] B. Witten, J. Shragge, "Quaternion-based Signal Processing," Stanford Exploration Project, New Orleans Annual Meeting, pp. 2862-2866, 2006.

[6] S. J. Sangwine, C.J. Evans, T.A. Ell, "Colour-sensitive edge detection using hypercomplex filters," Proc. 10th European Signal Processing Conf. EUSIPCO, Tampere, Finland, 2000, vol. 1, pp. 107-110.

[7] S.-C. Pei, Y.-Z. Hsiao, "Colour image edge detection using quaternion quantized localized phase," 18th European Signal processing conference (EUSCIPCO'2010), Aalborg, Denmark, August 23-27, 2010, pp. 1766-1770.

[8] S.J. Sangwine, T.A. Ell, "Colour image filters based on hypercomplex convolution," *IEEE Proc. Vision, Image and Signal Processing*, vol. 49, pp. 89-93, 2000.

[9] P. Denis, P. Carre, C. Fernandez-Maloigne, "Spatial and spectral quaternionic approaches for colour images," Elsevier, *Computer Vision and Image Understanding*, vol 107, pp. 74-87, 2007.

[10] P. Bas, N. Le Bihan, J.-M. Chassery, "Color Image Watermarking Using Quaternion Fourier Transform," Proc. ICASSP, Hong Kong, 2003, 4 pages.

[11] X. Wang, C. Wang, H. Yang, P. Niu, "A robust blind color image watermarking in quaternion Fourier transform domain," *J. Systems and Software*, vol. 86, no. 2, pp. 255-277, February 2013.

[12] M. Bahri, "Quaternion Algebra-Valued Wavelet Transform," *Applied Math. Sciences*, vol. 5, no. 71, pp. 3531-3540, 2011.

[13] S. Gai, G. Yang, S. Zhang, "Multiscale texture classification using reduced quaternion wavelet transform," *Int. J. Electronics and Communication*, vol. 67, no. 3, pp. 233-241, March 2013.

[14] R. Mukundan, "Quaternions: From Classical Mechanics to Computer Graphics, and Beyond," Proc. 7th ATCM Conf., 2002, pp. 97-106.

[15] J. Farrell, *Mathematics for Game Developers*, Premier Press, Inc., 2004.

[16] J. Funda, R.P. Paul, "A Comparison of Transforms and Quaternions in Robotics," Proceedings, IEEE Int. Conf. Robotics and Automation, Philadelphia, September 24-29, 1988, vol. 2, pp. 886-891.

[17] D. Andreis, E.S. Canuto, "Orbit dynamics and kinematics with full quaternions," Proc. of the American Control Conference, Boston, Massachusetts, June 30 – July 2, 2004, pp. 3660-3665.

[18] P. R. Girard, *Quaternions, Clifford Algebras and Relativistic Physics*, Birkhäuser, Basel Boston Berlin, 2008.

[19] W.R. Hamilton, *Elements of quaternions*, Longmans, Green and Co., London, 1866.

[20] T. Bülow, G. Sommer, "The Hypercomplex Signal – A Novel Extension of the Analytic Signal to the Multidimensional Case," *IEEE Trans. Signal Processing*, vol. 49, no. 11, pp. 2844-2852, November 2001.